

Modeling ocean processes below Fimbulisen, Antarctica

Lars H. Smedsrud,^{1,2} Adrian Jenkins,³ David M. Holland,⁴ and Ole A. Nøst⁵

Received 11 February 2005; revised 16 August 2005; accepted 20 October 2005; published 18 January 2006.

[1] Model simulations of circulation and melting beneath Fimbulisen, Antarctica, obtained using an isopycnic coordinate ocean model, are presented. Model results compare well with available observations of currents and hydrography in the open ocean to the north of Fimbulisen and suggest that Warm Deep Water exists above the level of a sub-ice-shelf bedrock sill, the principal pathway for warm waters to enter the sub-ice-shelf cavity. The model shows a southward inflow of Warm Deep Water over this sill and into the cavity, producing a mean cavity temperature close to -1.0°C . This leads to high levels of basal melting (>10 m/a) at the grounding line of Jutulstraumen and an average melting over the ice shelf base close to 1.9 m/a. The southward inflow is a compensating flow caused by the northward outflow of fresh, cold water produced by the basal melting. Results on inflow and melting are difficult to validate since no in situ measurements yet exist in the cavity. If such high melt rates are realistic, the mass balance of Fimbulisen must be significantly negative, and the ice shelves along Dronning Maud Land must contribute about 4.4 mSv of melt water to the Weddell Sea, about 15% of the total Antarctic meltwater input to the Southern Ocean.

Citation: Smedsrud, L. H., A. Jenkins, D. M. Holland, and O. A. Nøst (2006), Modeling ocean processes below Fimbulisen, Antarctica, *J. Geophys. Res.*, 111, C01007, doi:10.1029/2005JC002915.

1. Introduction

[2] Fimbulisen is the largest ice shelf in the northeastern Weddell Sea. An unusual feature that distinguishes it from most other Antarctic ice shelves is that, in places, it overhangs the continental slope [Nøst, 2004]. Even where it does not, the continental shelf north of the 200 m deep Fimbul ice front is at a maximum 40 km wide, meaning that the ice shelf is exposed to the Antarctic coastal current (Figure 1). This coastal current acts as a dynamic barrier, keeping the Warm Deep Water (WDW) of the Weddell Sea away from the ice shelf cavity by depressing the thermocline. WDW, defined by temperatures above 0°C , has a core temperature of 1°C . This warm water core is located just 100 km offshore of the ice front.

[3] It has been argued [Fahrbach *et al.*, 1994] that the close proximity between the ice shelves along Dronning Maud Land and the WDW leads to large basal melt rates, generation of significant volumes of near-surface freshwater, and hence suppression of deep-water formation in the eastern Weddell Sea. A recent circumpolar model study of most Antarctic ice shelves indicated that the freshening and cooling of the water masses due to melting of the ice

shelves has a large-scale impact on the Weddell Sea circulation, stratification, sea-ice cover, open-ocean convection, and deep-water characteristics [Beckmann and Goosse, 2003]. One coarse resolution model [Hellmer, 2004] has Fimbulisen contributing as much as 27% of the total melting of the major Antarctic ice shelves. Although this is likely to be an overestimate, resulting from an inability to resolve the narrow continental shelf in front of Fimbulisen [Hellmer, 2004], it does demonstrate how rapidly the ice shelf could melt if fully exposed to the offshore WDW.

[4] Some regional oceanographic features have been observed, but remain unexplained, including an eastward flowing undercurrent at 1000 m depth [Heywood *et al.*, 1998]. The coast and the continental slope are in close proximity, and it is not clear how the Antarctic coastal current and the Antarctic slope front current merge in the waters just to the north of Fimbulisen.

[5] Since 1950, the deep waters around Antarctica have been warming faster than the average of the global ocean waters [Gille, 2002]. In particular, the ocean heat content close to the continent along the Greenwich meridian has been increasing steadily over the last 25 years, close to 6 W/m^2 on average [Smedsrud, 2005]. This suggests that Fimbulisen may have been exposed to an ocean warming signal over recent decades.

[6] As the detailed topography of Fimbulisen and the cavity beneath it has been to date largely unknown, thus forestalling the application of a detailed numerical model, past studies have not shed much light on the details of the dynamic interactions between this ice shelf and the neighboring ocean.

[7] Using a newly available topographic data set [Nøst, 2004], we here apply a numerical model to the study of the

¹Bjerknes Centre for Climate Research, University of Bergen, Bergen, Norway.

²Also at Geophysical Institute, University of Bergen, Bergen, Norway.

³British Antarctic Survey, Cambridge, UK.

⁴Courant Institute of Mathematical Sciences, New York University, New York, New York, USA.

⁵Norwegian Polar Institute, Tromsø, Norway.

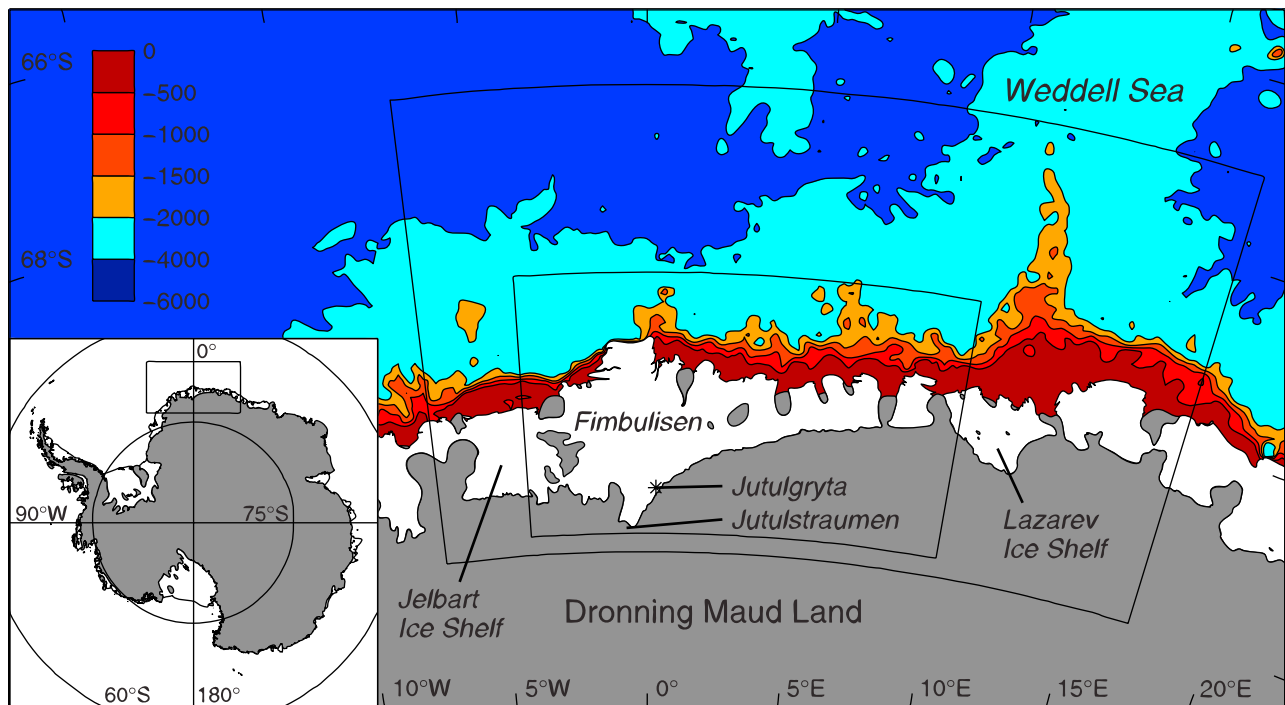


Figure 1. Map of Fimbulisen and the Weddell Sea. Floating ice shelves are shown in white, while grounded ice is shown in gray. Ocean bathymetry (m) is indicated by the colored shading. The extent of the model domain is shown by the outer box, and the inner box indicates the portion shown in subsequent figures (Figures 2, 3, 6, and 7).

ocean waters beneath and to the north of Fimbulisen, in order to investigate this dynamic interaction. The model is presented in section 2, followed by results in section 3 and a discussion in section 4. The central problem addressed in this study is how, and to what extent, WDW comes into contact with Fimbulisen and causes the ice shelf to melt. We seek to understand this inflow of WDW, and the mechanisms that act to suppress or enhance the inflow.

2. Model

[8] We apply the ocean and ice shelf models of the POLAIR (Polar Ocean Land Atmosphere and Ice Regional) modeling system to the area surrounding Fimbulisen with simplified atmospheric forcing. The ocean component of POLAIR is a version of the Miami Isopycnic Coordinate Ocean Model (MICOM) [Bleck, 1998], modified to allow for an ice shelf cavity [Holland and Jenkins, 2001]. The ocean model consists of a vertical stack of horizontal, shallow water layers, with each layer representing fluid of a constant density. For each layer a momentum, mass, temperature, and salinity equation is solved. The topmost layer, referred to as the mixed layer, is unique in that it can have a spatially varying density. Indeed this is necessary as this layer, being in direct contact with the overlying ice shelf base, receives variable fluxes of heat and freshwater. The heat and freshwater exchanges are formulated using a viscous-sublayer model [Holland and Jenkins, 1999].

[9] The model grid covers Dronning Maud Land between 7°W and 17°E as shown in Figure 1. The grid incorporates Fimbulisen, the Jelbart and Lazarev ice shelves, and reaches well north into the Weddell Sea to 67°S. Grid boxes are

locally square, and have a resolution of 0.25° in longitude. This means that the boxes increase from 8.8 km to 10.9 km, going from the southern to the northern boundary in the domain.

[10] A newly available, limited area, ice thickness and seabed topography data set [Nøst, 2004] was blended in with the existing, pan-Antarctic BEDMAP data set [Lythe and Vaughan, 2001] to produce the highest possible quality topography over the model domain (see Figure 2). The new data set covers the region 3°W to 6°E, and 70°S to 72°S, which forms only part of the larger domain of the model. We will discuss model results primarily within the smaller region. The Jelbart ice shelf covers the area west of Fimbulisen from 3°W and westward, while the Lazarev ice shelf covers the area east of 9°E.

[11] The sea floor topography is fairly complex. The most important topographic feature is a 570 m deep sill at 1°W and 70°S, visible in Figure 2. Water column thickness changes from 300 m at the sill up to a maximum of 800 m over the 1100 m deep basin to the south. Here we refer to the sill as the Jutul sill, and the basin as the Jutul basin. The Jutul basin connects with two other basins to the east through sills at ~500 m depth. These eastern basins also connect directly with the open ocean to the north, with the deepest sill at 3°E being 320 m deep.

[12] The ice stream Jutulstraumen, located close to the Greenwich meridian, carries the main ice discharge from Dronning Maud Land. It creates an elongated tongue of thicker ice that extends through the central part of the ice shelf. Over the Jutul basin the ice shelf base is found at about 400 m depth in the central part of Jutulstraumen, and at about 200 m depth on either side. A region between the

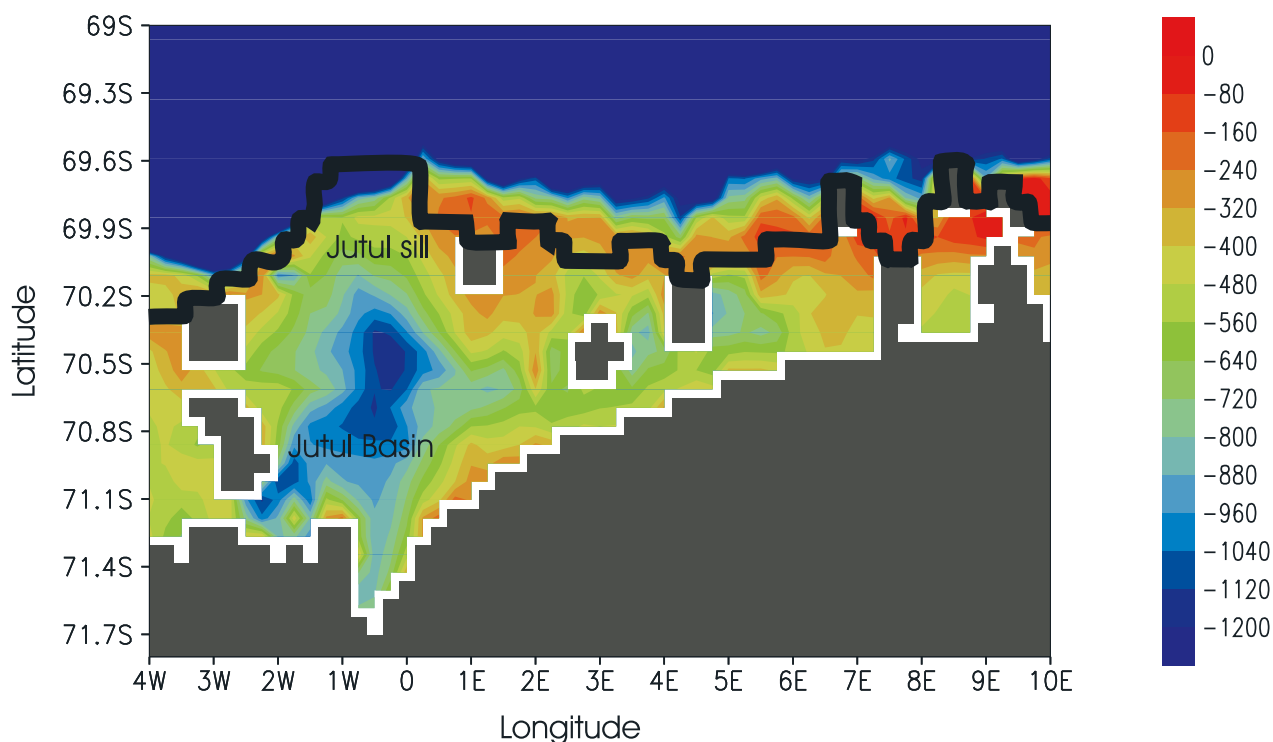


Figure 2. Ocean bathymetry (m) for central parts of the model domain as indicated by the inner box in Figure 1. Bathymetric shading is truncated at 1200 m to highlight the fine seabed features below Fimbulisen. North of the ice shelf and continental shelf the model bathymetry is physically truncated at a depth of 2500 m for computational efficiency. The ice front of Fimbulisen is indicated by the thick black line, and model grid cells, or resolution, are indicated by the fine detail, black land mask.

deepest part of the Jutul basin and the grounding line of Jutulstraumen has no topographic observations. To fill this data void, we interpolated the bedrock and ice shelf base along glacial flow lines. This construction leads to a channel connecting the 875 m deep grounding line and the basin.

[13] To resolve the various water masses, both inside and outside the sub-ice-shelf cavity, we used 16 isopycnic layers for the ocean model's vertical coordinate. For the less stratified deep water we assigned potential densities linearly interpolated between 27.80 and 27.85 kg/m^3 to the lower 8 layers. The minimum potential density of the surface layer was set to 27.10 kg/m^3 , and the upper 8 isopycnic layers were assigned densities linearly interpolated between this value and 27.80 kg/m^3 . On each isopycnic layer, the initial thickness, temperature, and salinity were obtained by projecting observational data from the Hydrographic Atlas of the Southern Ocean [Olbers *et al.*, 1992] onto the model layers. As no observational data exists in the sub-ice-shelf cavity, a horizontal extrapolation scheme was used to fill it. The scheme fills the cavity with waters on the freezing point at atmospheric pressure having the same density as those observed near the ice shelf front. Salinity was then recalculated to maintain the observed density profile.

[14] Along the western, northern, and eastern sidewalls of the domain we specified “sponge layers” of 5 model grid points width. Along these walls, the model temperature and salinity were restored toward the initialization fields. The restoring timescale was 15 days for the outermost grid points of the sponge layer, and 30 days for the innermost. This scheme ensures that properties at the boundary can be

kept close to observed values, without generating excessive gradients in the interior of the domain. The flows tangential and normal to the outermost perimeter of the model domain were specified as zero.

[15] We have chosen a fairly simple way to force the model dynamically. This reflects the lack of proper in situ time series observations to the north of the ice front. The topography of the region is also complex and clearly plays a first-order role in directing the wind and buoyancy driven flows. In order to isolate and understand the role of topography in permitting or preventing WDW access to the cavity beneath Fimbulisen we adopted external forcing with minimal complexity. We therefore apply an idealized easterly wind field that is constant in time. The westward speed of the wind is a cosine function of latitude, decreasing from 15 m s^{-1} at the southern boundary of the domain to zero at the northern boundary. This gives a wind speed of about 12 m s^{-1} just north of the ice front. As a model sensitivity study, a lower surface wind speed of 10 m s^{-1} (8 m s^{-1} at the ice front) is also included. Similarly, we did not include temporal variation in the WDW temperature, although observations suggest that it has warmed over the past two decades [Smedsrud, 2005]. We leave the subject of temporal trends in the circulation for future investigations, focusing here on a first description of the basic circulation pattern and an understanding of the underlying processes.

[16] The zero normal flow condition imposed at the eastern, northern and western boundaries of the domain is another simplification and is clearly unrealistic. Other strategies would clearly have been possible, such as allow-

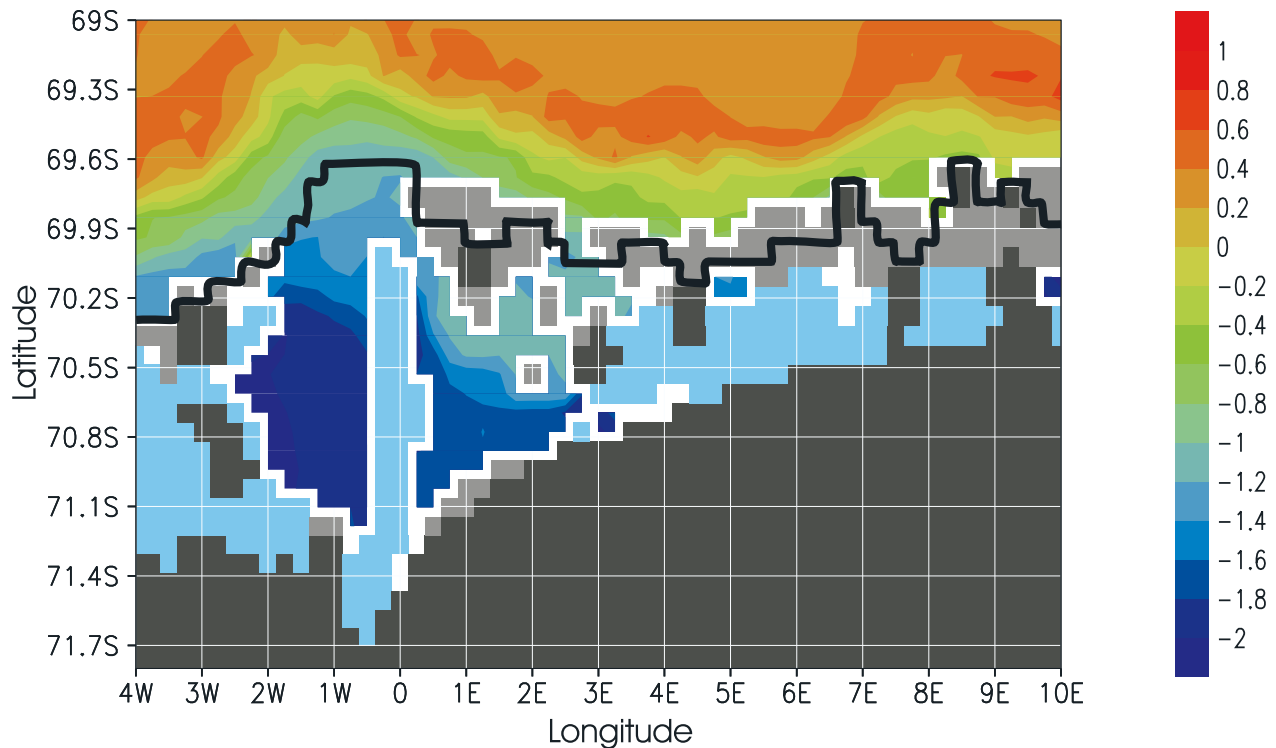


Figure 3. Annual mean potential temperature ($^{\circ}\text{C}$) at 300 m depth in the steady state solution (year 11). Fimbulisen is shown in light blue, and the ice front as the thick black line. Open ocean depths shallower than 300 m are shown as light gray. See Figure 1 for location.

ing recirculation in a separate channel or applying cyclic boundary conditions in the east and west. However, these strategies carry with them the danger that an influence of the ice shelf could be recirculated into the coastal current upstream of Fimbulisen. Our solid boundaries force recirculation in the northern parts of the domain, beyond the region of interest in this study, but continuous restoration to observations throughout the process ensures that all influence from the ice shelf is lost before the waters re-enter the coastal current in the east. Our results show that this simple strategy does produce a realistic current along the coast and slope at the Greenwich meridian that compares well with recent observations [Klatt *et al.*, 2005].

[17] Observations show that the area of the model domain is covered by a mean sea ice concentration between 40 and 60% [Zwally *et al.*, 2002]. The maximum concentration is around 90% in September, and the area is largely ice free during January–March. We have chosen not to apply the sea ice module of the POLAIR system in line with the simplified approach described above. The sea ice cover moves westward with the mean wind and currents, and thus transfers the wind stress to a large, but unknown, degree. We approximate the natural condition by applying the wind stress directly to an open-ocean domain.

[18] The main additional effects of the sea ice are to keep the sea surface temperature close to freezing, and drive a seasonal change in the sea surface salinity. During the ice free months the temperature increases in the surface layer to a maximum of about 3°C , but there is always a layer close to the freezing point present down to around 150 m depth. During earlier model simulations [Smedsrud *et al.*, 2005] a seasonally varying temperature field was applied. This had

no effect on Fimbulisen or the nearby circulation, so in the runs presented here we apply an open-ocean surface temperature restored to the in situ freezing point all year round.

[19] Open-ocean surface salinities were restored toward a constant value for the domain. For the mean state we focus on here, a sea surface salinity of 34.3 was used throughout the year based on Olbers *et al.* [1992]. Model runs using a sinusoidally varying field with a summer minimum of 33.9 in March, increasing to 34.4 in September, are included to indicate model sensitivity. The restoring timescales for temperature and salinity were both set to 30 days.

3. Results

[20] The model was run for 11 years of simulated time, being forced by the wind, temperature, and salinity fields as described earlier. After about 4 years of integration the model reached a steady state. The mean cavity temperature increased from the initial -1.9°C over 3 years to around -1.0°C , then deviated by less than 0.05°C from this value over any year in the steady state situation. Most of our results are presented from a “steady state” situation in model year 11, averaged over the full year. This mean situation is our main focus, and when maximum, minimum, or mean values are referred to below, they usually describe spatial properties specifically below Fimbulisen, here taken to be the area south of the ice front between 3°W and 7°E of Figure 3.

[21] In the two last subsections (3.4 and 3.5) we also present results on the model variability in time and on its sensitivity to changes in the simplified surface forcing. For the “steady state” results there is no yearly variation in

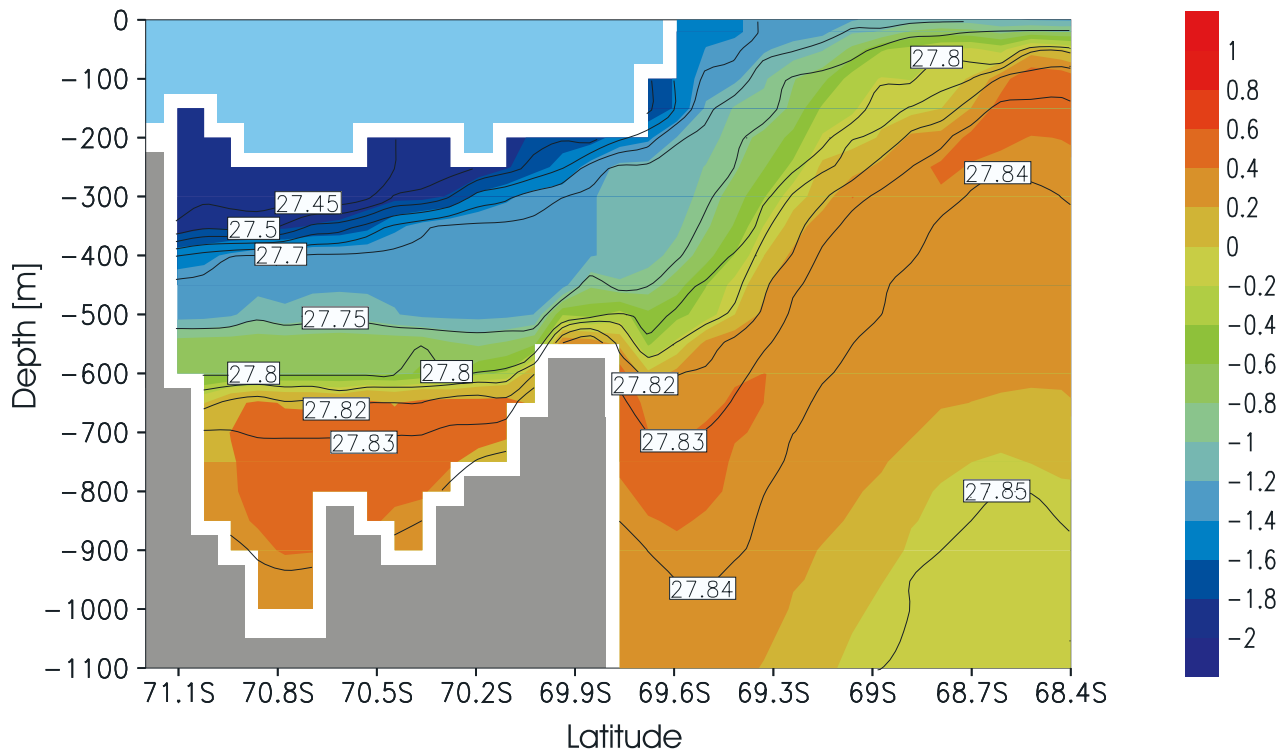


Figure 4. Annual mean potential temperature ($^{\circ}\text{C}$) along 1°W in the steady state solution (year 11). Fimbulisen is shown in light blue, and the bedrock in gray. Potential density contours, which parallel layer interfaces, are shown as black lines.

forcing, so the variability is solely produced internally in the model. The varying sea surface salinity causes yearly fluctuations in the cavity and is included as a contrast to the “steady state” results.

3.1. Hydrography

[22] Figure 3 is a horizontal slice of the potential temperature field at a depth of 300 m. It illustrates that WDW, at this depth horizon, is confined to the region north of the continental shelf break, away from any direct contact with the ice shelf. Patches of ice shelf melt water (indicated by the low temperatures) are found south of the ice front, and follow the general westward flow along the continental shelf when they reach the ice front. The colder water in the south has a salinity below 34.4 (not shown), and is less dense than the WDW with its salinity of 34.65. The resulting thermohaline structure helps to strengthen the westward flow of melt water near the surface.

[23] Figure 4 shows a vertical section of potential temperature along 1°W . It reveals the vertical structure of the dominant water masses. It is taken at the longitude of the Jutul sill (Figure 2). The core of the WDW north of the ice front is shallower than the 570 m deep sill, but it deepens rapidly as the continental slope is approached. Below the ice shelf there is a 100 m thick layer of water colder than the surface freezing point (-1.88°C for a salinity of 34.25). This is Ice Shelf Water (ISW), cooled to the in situ freezing point by the melting of the ice shelf above it. Waters with temperatures above 0°C enter the cavity as part of a deep, more saline inflow that compensates the shallow outflow of fresh, cold water, producing a kind of estuarine circulation pattern within the cavity.

[24] The vertical structure in salinity (not shown) mimics that of temperature, so that the lowest temperatures correspond to the lowest salinities, and the warmest waters are the most saline. Salinity dominates the density structure at these low temperatures. However, in the deepest layers, below the WDW, the larger thermal expansion coefficient of the colder water means that at these pressures the decrease in salinity and temperature with depth produces a stable water column as seen in Figure 4.

[25] The stratification is such that the isopycnals essentially follow the isotherms in Figure 4. Thus, in the upper layers, the isopycnals deepen as they approach the coast from the north. This descent of the upper isopycnals reflects the presence of the relatively fresh coastal waters. In the lower layers, the isopycnals rise as they approach the continental slope from the north. This rise of the lower isopycnals brings water warmer than 0°C to the depth of the Jutul sill, where it can enter the sub-ice-shelf cavity.

[26] The depth of the 0°C isotherm at the top of the WDW core is not constant along the ice front. In Figure 4 it is close to 500 m at 1°W and 69.77°S . At this same latitude between 1 and 7°E the upper 0°C isotherm is as shallow as 350 m in places, but it remains below the level of the continental shelf, which east of the Jutul sill has a maximum depth of 320 m.

[27] The mixed layer beneath the ice shelf has a maximum thickness of 240 m along the western side of Jutulstraumen. Salinities reach a maximum of 34.4 at the grounding line of Jutulstraumen and along its deeper parts, and a minimum of 33.35 in an area around 3°W close to the ice rise features. The minimum temperature in the mixed layer, below the ice shelf, is -2.18°C , which corresponds to

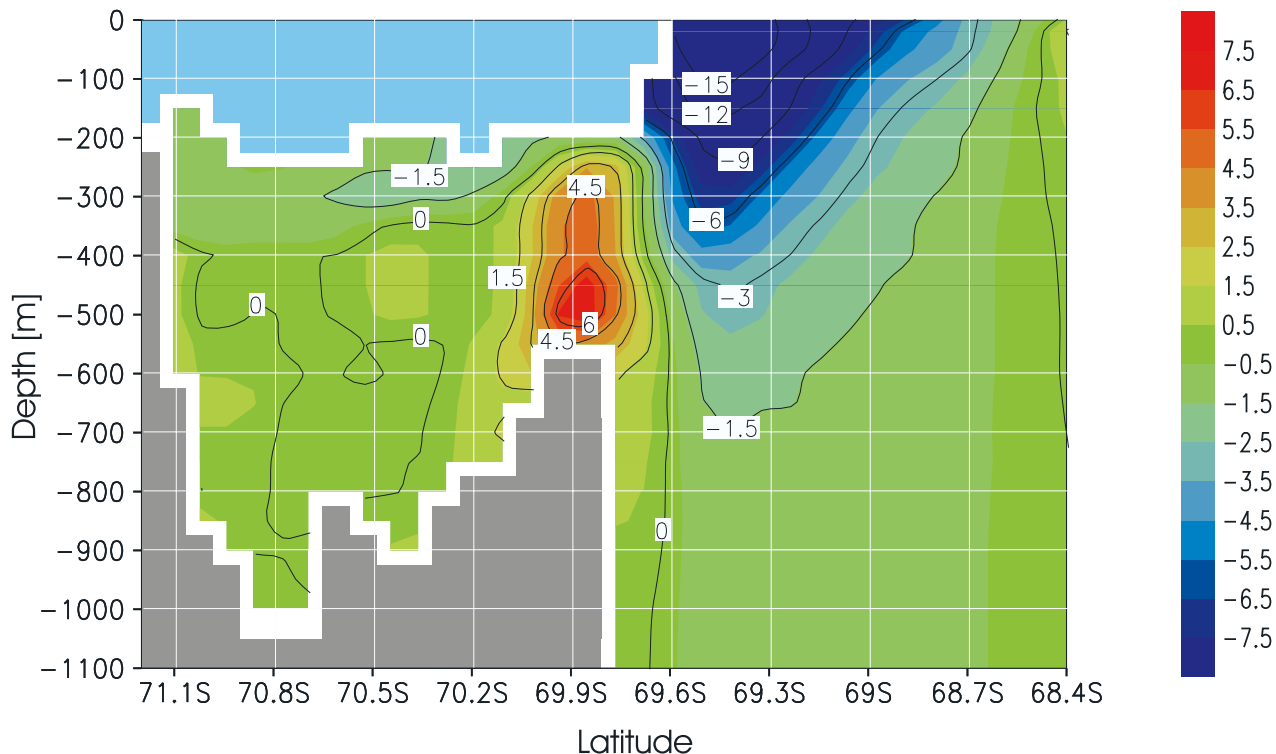


Figure 5. Annual mean eastward current speed (cm/s) at 1°W in the steady state solution (year 11).

the freezing point in situ for waters in the depth and salinity ranges of the mixed layer. The mixed layer below Fimbulisen reaches a maximum temperature of -0.86°C at the grounding line of Jutulstraumen. These properties reflect the circulation and basal melting that occurs beneath the ice shelf as described in the following sections. The annual mean cavity-averaged temperature is -0.97°C , and the average salinity is 34.43.

[28] The open-ocean mixed layer reaches a maximum thickness of 340 m in the southwestern corner of the domain, where a homogeneous layer of fresh, cold water exists as a result of the glacial melting occurring further east. Although this pool is an artifact of our closed domain, its presence has no adverse impact on the simulation because it is located well downstream of the ice shelf cavity.

3.2. Circulation

[29] A westward coastal current follows the ice shelf front, flowing as shown in the north-south vertical transect of Figure 5. It has a small component of 1 cm/s that is associated with the surface slope (barotropic and constant with depth), and a maximum speed of 19 cm/s close to the surface. The decrease in velocity with depth is geostrophically related to the downward slope of the isopycnals (toward the south) in the upper part of the water column. The total transport of the coastal current between the coast and 68.5°S is 7.5 Sv, of which 4 Sv is the modeled barotropic part.

[30] The increasing density northward (Figure 4) gives rise to an increase in eastward speed when moving downward through the water column (i.e., from the thermal-wind relation). This separates the westward flowing fresher and less dense coastal current from the denser (warmer and saltier) water masses below. This westward flowing coastal

current is well developed in the model west of 14°E , and stretches northward about 100 km from the ice shelf front. Eddies drift westward within it causing the current to meander. The flow north of 68.5°S is primarily eastward, returning the westward flow of the southern part of the domain.

[31] A strong eastward flow at the level of the Jutul sill is a robust feature of the simulation (see Figure 5). This current follows the bathymetry of the Jutul basin south of the ice shelf front between 1°W and 2°E , and is the primary source of water flowing into the cavity beneath Fimbulisen. The increase in eastward current speed with depth is in thermal-wind balance with the downward sloping isopycnals toward the south in the upper layer. This downward slope of the isopycnals in the upper layer follows the isotherms shown in Figure 4.

[32] The upward sloping isopycnals and isotherms (toward the south) in the bottom layer and lower part of the water column are a permanent feature along the continental slope. If it were not for this upward trend there could be no southward flow of warm water up and over the 570 m deep Jutul sill at the northern entrance to Jutul basin. Although the upper boundary of the WDW is found above this depth horizon well north of the ice front, at only 25 km to the north of the sill it is below this level (see again Figure 4). We suggest some likely mechanisms explaining the undercurrent and the upward sloping isopycnals in section 4.3.

[33] The flow across the Jutul sill is shown at a depth horizon of 450 m in Figure 6. The current at the sill oscillates between 6 and 10 cm/s in strength, with a southward component close to 5 cm/s. The 380 m ice draft of Jutulstraumen serves as a further topographic control, guiding the inflow southward toward the grounding line of

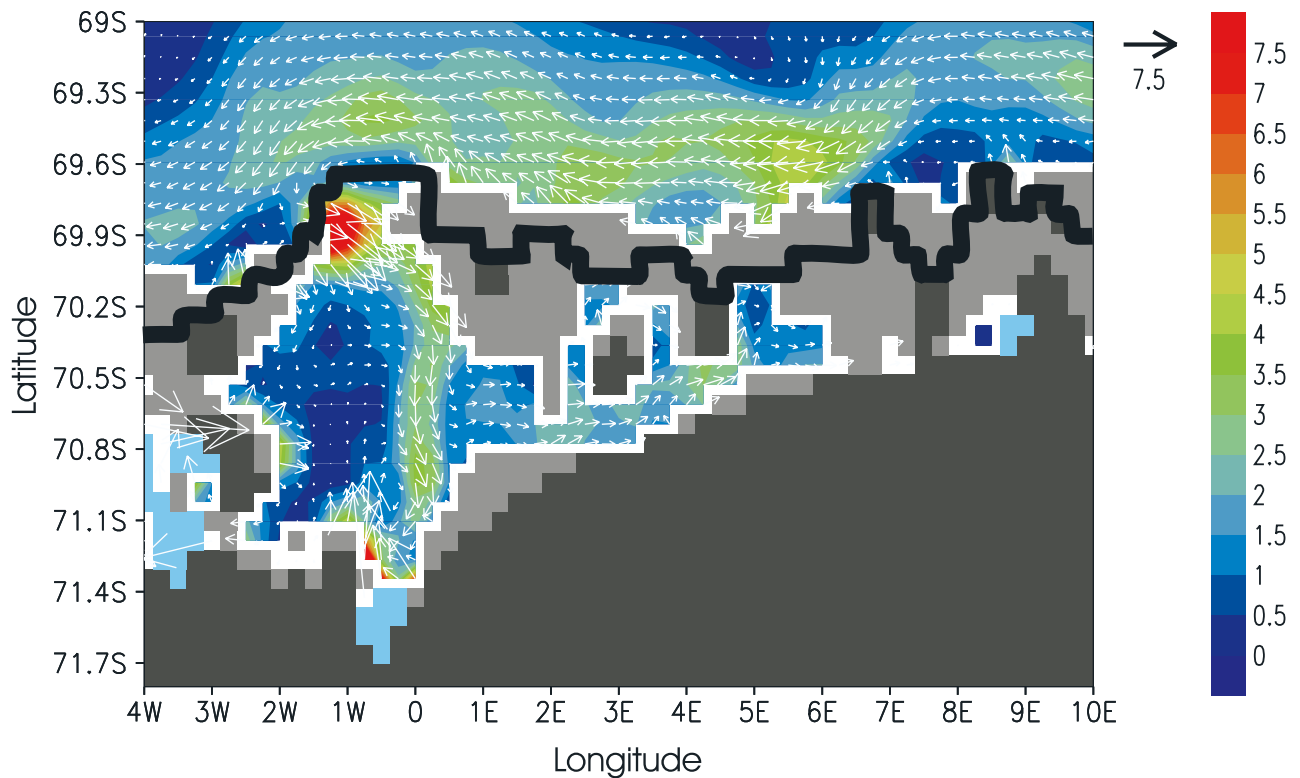


Figure 6. Annual mean flow at 450 m depth in the steady state solution (year 11). The color scale shows current magnitude (cm/s) and the arrows are current vectors with a 7.5 cm/s arrow to scale in the upper right corner. The thick black line is the ice front of Fimbulisen, and location is shown in Figure 1.

Jutulstraumen. The overall inflow beneath the ice shelf is 3.3 Sv.

[34] Melt water flows out of the cavity along the western “coast” of the basin starting at 600 m depth near the grounding line, and rising to 350 m depth at the ice front. Some of the melt water escapes the cavity through shallow tunnels between the ice rises located to the west and contributes to the westward flowing waters in the upper 100 m layer (see Figure 5).

[35] Flow in the mixed layer within the cavity is mostly directed northward. Average speeds are in the range 2–5 cm/s with a maximum close to the grounding line of Jutulstraumen of 10–15 cm/s, partly visible at the 450 m depth horizon in Figure 6. West of Jutulstraumen the flow is northwest, and east of Jutulstraumen the flow is directed north, as dictated by the change in water column thickness.

3.3. Basal Melting

[36] During the model setup procedure the water within the cavity is assigned a temperature equal to the surface freezing point for its salinity. The mean basal melting steadily increases from an initial value around 0.6 m/a as warmer waters begin to penetrate the cavity. Inflow of WDW beneath an ice shelf can cause high basal melting rates. Figure 7 shows that the melt rates close to the grounding line of Jutulstraumen, 450–875 m depth, reach more than 14 m/a over a large area, the absolute maximum being 65 m/a. One particular small area has sustained melt rates above 40 m/a, while the average over the more expansive inner 900 km² (9 grid boxes) of Jutulstraumen is 10 m/a. Within model year 11 the

mean melting of Fimbulisen (the area shown in Figure 7) is 1.93 m/a.

[37] An area with melt rates above 14 m/a is also found to the east, on the ice shelf around 4°E where the ice shelf draft is about 400 m. There, efficient melting is caused by a relatively warm temperature in the mixed layer of -1.3°C . There is no direct inflow over the nearby sill, so the elevated temperature seems to be caused by the inflow above the Jutul sill, and subsequent topographic guidance around the cavity (Figure 6). This is the first part of the ice shelf base that entering water masses at the 350 m depth level encounter. Elsewhere below Fimbulisen, the fresh, cold mixed layer waters usually isolate the ice shelf base from direct contact with the WDW.

[38] Only minor areas grow marine ice. The maximum rates, found close to the ice front, are 5 m/a, and are caused by the outflowing ISW and the associated pressure release as the ISW rises along the shoaling ice shelf base. The aforementioned minimum temperature below the ice shelf of -2.18°C , found just north of the deepest part of the Jutulstraumen grounding line, has associated with it a small patch of 0.2 m/a growth of marine ice.

[39] The melting pattern results in a net melt water flux from the ice base to the ocean. For Fimbulisen between 3°W and 7°E this fresh water flux is close to 3.0 mSv. If we include the remaining ice shelf area of the model domain, i.e., the Jelbart and Lazarev ice shelves, this increases to 4.4 mSv.

3.4. Model Variability

[40] The properties described above represent our best estimate of the mean state of Fimbulisen and the nearby

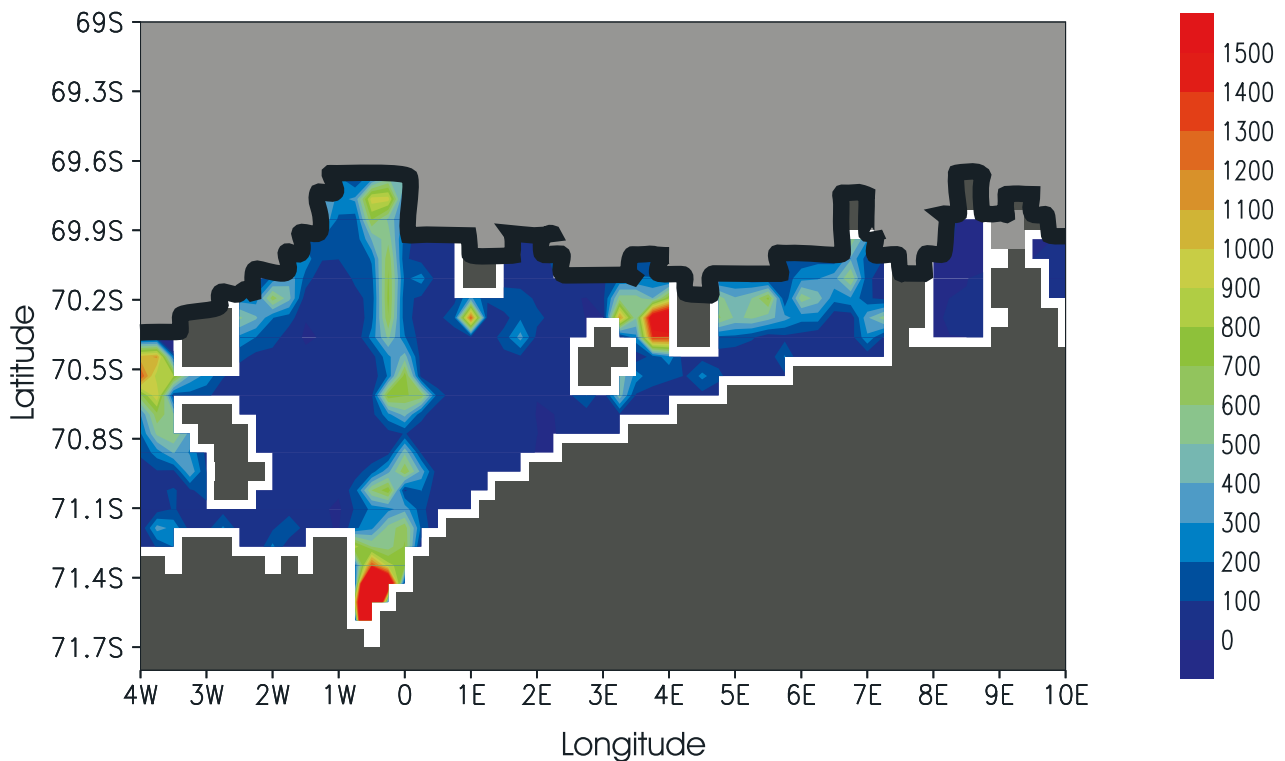


Figure 7. Annual mean basal melting (cm/a) below Fimbulisen in the steady state solution (year 11). See Figure 1 for location.

slope. Most of the numbers quoted above were averaged over a full year, but the model has significant internal variability on shorter timescales. The mean situation in model year 11 did not have any annual variation in forcing, so the modeled variability reflects internal processes in the model that are, to a large extent, connected with meandering in the coastal current. This brings water masses of varying temperature and volume into the cavity, and leads to varying melting, and thus fresh water fluxes.

[41] The spatially averaged temperature of the cavity varies by $\pm 0.02^\circ\text{C}$ from the annual average value of -0.97°C . Salinity of the cavity varies in a similar manner by ± 0.005 about the mean of 34.43 throughout the year. There are no clear modes in the variability, but higher temperature and higher salinity occur at the same time, and the fluctuations last from a couple of weeks to several months.

[42] The temporal variation of the spatially averaged melt rate for the ice shelves within the domain (Fimbulisen, Jelbart and Lazarev ice shelves) is shown in Figure 8 as the “high wind, constant SSS” case. In order to compare other model runs with different forcing, results are plotted for model year 5 in all cases, but the variability apparent in year 5 of the standard run is very similar to that in year 11, discussed thus far. After year 4 of the simulation the maximum net melt rate is 2.34 m/a, and the minimum melt rate is 1.16 m/a. The variability of the melt rate is typically ± 0.1 m/a over a timescale of around a week. The variability over a weekly timescale for the mean total fresh water flux of the domain is ± 0.2 mSv, while the total range after model year 4 for this fresh water flux is 3.5 to 5.6 mSv.

3.5. Model Sensitivity

[43] Earlier model simulations without any wind forcing gave a shallower WDW core at the sill level. This led to more WDW making it directly into the cavity, and a larger basal melt rate. Weaker westward winds thus tend to increase ice shelf melting along the coast.

[44] The effect of lower westward wind speed is clearly shown in Figure 8 where the “low wind, constant SSS” curve shows basal melt rates from a model run having 8 m/s winds at the coast instead of the 12 m/s in the standard run. This increases the mean net melt rate by 1.6 m/a.

[45] A similar increase in net melt rate is caused by applying a surface salinity that varies sinusoidally from a minimum of 33.9 in March to a maximum of 34.4 in September. This is the “high wind, varying SSS” curve in Figure 8. The small peak in net melting in the autumn is associated with a peak in the mean cavity salinity, and a peak in cavity temperature a month earlier, so the surface salinity increase directly influences the water masses below Fimbulisen.

[46] A combination of both lower wind speed and a varying sea surface salinity leads to much stronger, and probably unrealistic levels of basal melting, this is the “low wind, varying SSS” curve in Figure 8. The mean melting of the domain reaches 5 m/a, and the seasonal signal is now much stronger. In this case the cavity temperature and salinity vary in line with the net melting. The maximum melting occurs in early May with the salinity maximum a month earlier, and a temperature maximum a month later. The main reason for the large melt rates and a higher mean cavity temperature of -0.46°C is the shallow level of the WDW core near the sill. In this case the 0°C isotherm rises

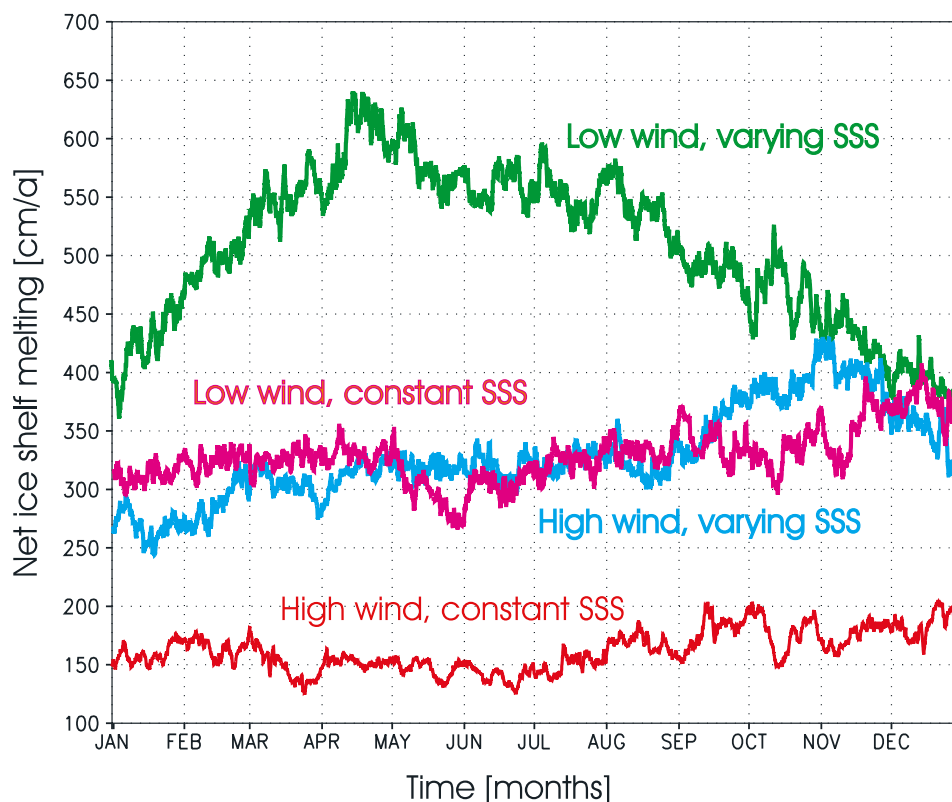


Figure 8. Model net melt rate for the whole domain during model year 5 for different model forcing. The standard run referred to in most cases is the “High wind, constant SSS” run. The other runs are discussed in the text.

to a depth of 400 m, some 200 m above the sill, and the WDW fills a further 200 m of the cavity beyond that shown in Figure 4 for the standard case. This high melting case was run through to model year 11, and also showed a stable annual cycle after model year 4.

4. Discussion

[47] Despite the fact that the model domain covers a relatively small geographical area, and that a “no flow” condition is specified at the outermost perimeter, the restoration to observation at the boundaries produces a realistic distribution of water masses along the continental slope north of Fimbulisen. Water properties there should exert the primary control on the mass balance of the ice shelf. We do not expect the model to describe the large-scale circulation patterns, like the flow of the Weddell Gyre, but the simplified wind stress employed creates a sufficiently realistic westward surface flow, and a southward Ekman transport of fresh, cold surface waters toward the ice front. Melting is fundamentally controlled by how much of the underlying WDW accesses the cavity.

4.1. Cavity Validation

[48] The only available CTD data from beneath Fimbulisen are casts in Jutulgryta, a crevasse adjacent to Jutulstraumen at 71.3°S , 0.25°E (Figure 1). Below a 10 m layer of sea ice and a 30 m layer of slush, observed temperatures were close to the freezing point down to 300 m depth [Orheim *et al.*, 1990]. The measured temper-

ature range was -1.98 to -1.94°C with salinities close to 34.3, including data from both 1990 and 1991 [Østerhus and Orheim, 1992]. Local freezing processes in the crevasse probably govern the temperature profile above the 300 m depth level of the surrounding ice base, much as the model results of Khazendar and Jenkins [2003] indicate.

[49] In the waters below, the observed temperature and salinity increase downward, confirming the influence of warmer and more saline water masses beneath the ice shelf. Maximum values at the 400 m deep ocean floor are -1.8°C and 34.35. A six month temperature series taken at 370 m depth showed intrusions of warmer water up to -1.7°C [Østerhus and Orheim, 1992]. The presence of warmer waters at depth compares qualitatively with model results. However, at 0.25°E the model results show a temperature increase from -1.8°C at the 200 m deep ice base to -1.2°C at a depth of 400 m; similar to results shown in Figure 4 for the 1°W section. The Jutulgryta feature is fairly close to the grounding line, being about 10 km distant, and the local bathymetry is steep. On the model grid the seabed depth changes by 400 m between adjacent points, so this site is not an optimal one for validation. How representative the lower 100 m in Jutulgryta are of the rest of the sub-ice-shelf water masses remains an open question. For the moment then, lacking sufficient observations, the model results of temperatures below 400 m depth beneath Fimbulisen in general cannot be validated.

4.2. WDW Upper Extent

[50] A key feature of the model simulations, is the depression of the main thermocline offshore of the conti-

mental shelf. The greater the depression the less likely that WDW can enter the cavity via the Jutul sill. This depression is primarily a consequence of the westward wind stress as noted by [Sverdrup, 1953]. The idealized westward wind stress applied in the model appears to satisfactorily mimic the real winds in this regard.

[51] The model simulations with weaker wind forcing gave shallower WDW, and larger basal melting. Stronger westward winds thus tend to decrease ice shelf melting along the coast.

[52] As a consequence of the northward advance of the ice shelf front in recent decades, some earlier shipborne CTD casts have actually ended up beneath where Fimbulisen sits today. A profile from January 1979 [Foldvik *et al.*, 1985] at 69.8°S, 1.2°W and 2166 m depth shows that the 0°C isotherm was at 589 m depth. This is the upper boundary of the WDW layer, and we use this height as a critical parameter to evaluate the model results. The model WDW upper boundary varies between 550 and 650 m depth through the year for this location, only 20 km north of the Jutul sill.

[53] While the comparison is encouraging, we note that the observed upper boundary of the WDW varies substantially with distance along the coast, and is also likely to vary in time at any location. In August 1986 the upper boundary of the WDW was at 375 m (69.5°S, 0.3°W and 1852 m depth), yet in June 1992 it was at 942 m at a site in between the two previous stations (69.7°S and 0.7°W, 2080 m depth). East of the Jutul sill the upper boundary of the WDW was found at 512 m at 2.7°E in February 2001 (69.9°S and 977 m station depth, [O'Dwyer, 2002]).

[54] The WDW core values observed during a February 2001 station at 627 m depth were 0.75°C for the temperature maximum, and 34.65 for salinity. Model WDW core values are 0.55°C and 34.69 at 550 m depth, so the modeled water mass distribution north of Fimbulisen seems reasonable. As noted by Robertson *et al.* [2002] the WDW has been steadily warming since the occurrence of the Weddell Polynya event during 1974–1977. Smedsrud [2005] found that the warming is indeed continuing along the coast with the highest heat content and core temperatures occurring along 69°S in 2001, on the Greenwich meridian north to 60°S.

4.3. Coastal and Undercurrent

[55] In general, observations show that along the coast the depth of the WDW core deepens from about 400 m far away from the coast to below 600 m above the continental slope [O'Dwyer, 2002]. This is in agreement with the model results shown in Figure 4. The general deepening of the WDW toward the coast is probably caused by downwelling at the coast driven by the westward winds as noted above. The westward winds create an onshore surface Ekman flux [Sverdrup, 1953] that causes the sea surface to rise toward the coast. This surface tilt is in geostrophic balance with a westward flowing barotropic coastal current, a feature captured by the model in Figure 5.

[56] The shape and magnitude of the coastal current in Figure 5 is similar to calculated currents based on 4.5 years of current-meter data and 5 sections observed between 1992 and 2001 [Klatt *et al.*, 2005]. The southernmost rig was placed in 2000 m depth at 69.4°S (instruments at 240 m,

745 m and 1950 m), and the coastal current clearly extends as far north as this position where water speeds in excess of 5 cm/s were recorded. The next current meter northward at 69.0°S and 219 m depth is at the northern limit of the coastal current both in the model results and in the observations [Klatt *et al.*, 2005].

[57] Few measurements exist on the continental shelf close to Fimbulisen, so the modeled flow cannot be validated directly there. The mean westward velocity for the upper 133 m at 7°W, in a water depth of 733 m, was 25 cm/s during 11 days in 2001 [O'Dwyer, 2002]. Observed iceberg drift speeds in the coastal current within the model domain, calculated from positions every 25 days, have a range of 11–23 cm/s [Young, 1998]. Icebergs have a typical draft of 200–350 m and their drift reflects the mean ocean velocities over this depth range.

[58] At 17°W Heywood *et al.* [1998] calculated a barotropic westward flow around 10 cm/s about 100 km north of the shelf break, and the main westward flow had a speed of 30 cm/s. Fahrbach *et al.* [1994] found the coastal current to have a mean speed of 10–13 cm/s based on a monthlong record about 100 km downstream of the 17°W section of Heywood *et al.* [1998].

[59] Altogether, this indicates that the model captures the main structure of the barotropic flow in the coastal region as shown in Figure 5, and that the modeled westward surface component of 18 cm/s is quite reasonable.

[60] The strongest eastward current in the model results is found at sill depth in Figure 5. This flow is typical for the sill area centered around 1°W (Figure 6). West of 2°W and east of 1°E the model shows a weak eastward undercurrent similar in structure to the undercurrent observed by Heywood *et al.* [1998]. The 17°W section included shipborne ADCP data and showed a current core flowing northeast at 4.6 cm/s at 800 m depth. The overall transport was 0.13 Sv in the undercurrent, which was trapped very close to the slope and was no more than 20 km wide and 500 m in depth.

[61] At 100 km further west Fahrbach *et al.* [1994] also found an undercurrent flowing northeastward, in this instance between 1000 and 1500 m depth, with a speed of 4 cm/s, while the 11-day current meter record from 7°W at 733 m depth [O'Dwyer, 2002] showed a mean eastward flow of 5 cm/s. Thus an eastward undercurrent seems to be present in the observations, and shallowing in depth toward Fimbulisen.

[62] In general the westward surface flow decreases with depth giving an eastward flow near the bottom. The flow is mainly controlled by the geostrophic balance and the westward decrease (or eastward increase) of the flow with depth is in agreement with the thermal wind relation and a southward decreasing density. A southward density decrease is generally found along the Dronning Maud Land coast. This is due to glacial melting and surface waters being blown onshore by the westward winds. As the decreasing westward velocity with depth is given by the thermal wind relation this is probably a general feature along the coast.

[63] The strongest eastward flow in the model is found south of the ice shelf front (Figure 5), and not over the continental slope. This flow structure may have been caused by the onshore Ekman flux being blocked by the ice front.

This will cause a sea level maximum at the ice front resulting in eastward flow south of the ice front and westward flow north of the ice front. This flow pattern is in agreement with the quasi-geostrophic analysis of flow near an ice shelf edge given by *Clarke* [1978].

[64] Near the bottom on the continental slope the isotherms are sloping upward toward the south bringing warm water up to the sill depth. This can be seen both in the model results (Figure 4), and in observations where the WDW upper boundary rises from 680 to 530 m depth over the 10 km nearest the coast [*Nøst*, 2004]. In this area of general wind-driven downwelling another process must be responsible for bringing the WDW up along the continental slope. It cannot be caused by the mean geostrophic currents, as these are nondivergent and cannot create any vertical velocities.

[65] We suggest two possible mechanisms for the upward sloping isopycnals. The first, and most straightforward, is simply the bottom upslope Ekman transport that occurs in areas with eastward near-bottom flow. These eastward undercurrents seem to exist because of the presence of a fresher, lighter upper layer. This upper layer has the north-south structure it does partly because of the westward wind stress, but also because of the effect of ice shelf melt water. We argue then that the eastward undercurrent could lead to WDW being transported upslope as a southward Ekman flow, over the Jutul sill, and thus lead to higher melting. This in turn would lead to a stronger eastward near-bottom flow, a stronger upslope WDW flow, and could be a positive feedback mechanism of the deep-water (continental-slope) ice-shelf system.

[66] The upward sloping isopycnals on the continental slope may also be caused by time-varying flow interacting with the mean flow over sloping topography. This effect has recently received attention, motivated by observations of deep recirculations around deep basins and sea mounts. An overview of the effect is given by *Adcock and Marshall* [2000]. *Greatbatch and Li* [2000] studied the effect of eddy parameterizations and found that some may lead to upslope flux of tracers over topography, similar to our results.

[67] *Fahrbach et al.* [1994] also found significant cross slope flow at 20°W. Typical observed flow toward the ice shelf in this region was ~ 1 cm/s along the bottom, where the water temperature was -1.2°C . Flow was generally away from the ice shelf in the upper layer. The estimated heat flux toward the ice shelf, based on these observations, was equivalent to 2.3 m/a of melting for a 75 km width of ice shelf.

[68] Our model results for inflow and melting below Fimbulisen are thus similar to observational results obtained further west. Even though there are no measurements of inflow below Fimbulisen, or any data confirming the upward sloping of isopycnals toward the south there, in the context of the regional observational database, the model results appear reasonable.

4.4. Basal Melting and Fresh Water Fluxes

[69] Melt rates beneath Fimbulisen have been previously estimated using remote sensing and coarse-resolution numerical models. *Rignot and Jacobs* [2002] found average basal melting of 4 ± 3 m/a for a 400 km² region close to the grounding line of Jutulstraumen, using satellite radar inter-

ferometry for ice motion and satellite radar altimetry to infer ice thickness. *Beckmann and Goosse* [2003] estimated an average of 3.7 m/a for the combined northeastern Weddell ice shelves, and *Hellmer* [2004] estimated 4.9 m/a for Fimbulisen, both using circumpolar models. The authors of these latter two studies considered their results to be overestimates owing to insufficient resolution of the narrow continental shelf in the model grids. Our estimates are an average melting rate of 1.9 m/a with a maximum at the grounding line of 65 or 10 m/a, depending on the area in question (~ 100 km², which is the grid box size, or ~ 1000 km², respectively).

[70] The inflow of WDW beneath the ice shelf is dependent on topography, and a coarse-resolution model could easily allow too much WDW into the cavity. Ours is the first regional, high-resolution model study of Fimbulisen and the first to use the new topographic data of *Nøst* [2004], and so we have an increased degree of confidence in our results as compared to those of previous coarse-resolution models. The model runs using weak wind forcing and a seasonally changing sea surface salinity show that Fimbulisen may transfer into a state of more efficient melting. On the basis of the available hydrography we find that Fimbulisen is not in this state at present.

[71] The overall fresh water flux from all Antarctic ice shelves is ~ 29 mSv according to *Hellmer* [2004] and *Beckmann and Goosse* [2003]. Our modeled mean fresh water flux for the domain around Fimbulisen, 4.4 mSv, is thus around 15% of the total Antarctic ice shelf melting. This estimate is close to 50% of the previous estimates for the same area as covered by the coarse resolution models. Our fresh water flux is comparable with the estimated fluxes from the two largest Antarctic ice shelves; Filchner-Ronne (3.7 mSv) and Ross (5.6 mSv).

[72] To put our modeled basal melting rate into a wider context we consider the various volume flux contributions that make up the local volume balance of Fimbulisen. We thus exclude the surrounding ice shelves of the model domain. Our modeled mean basal melting for Fimbulisen only is equivalent to a volume flux loss of 95 km³/a. The estimated volume flux gain from the discharge of Jutulstraumen is 13 km³/a [*Rignot and Jacobs*, 2002].

[73] Balance flux calculations using methods based on *Budd and Warner* [1996] suggest that a north flowing ice stream enters Fimbulisen around 7°E carrying 5 km³/a (Roland Warner, ACE CRC, personal communication, 2004), although some of this flow may be shared with the small ice shelf immediately to the east. The balance flux calculations also suggest a total outflow from the continent of approximately 33 km³/a between 3°W and 8°E if the grounded ice sheet is in balance with the present accumulation.

[74] Precipitation on Fimbulisen is also significant; an estimated flux is 14 km³/a based on snowfall observations [*Isaksson et al.*, 1999], and the area of Fimbulisen as used in this study ($\sim 50,000$ km²). Even without the additional loss from iceberg calving, for which we have no reliable estimate, it is clear that in net terms our modeled melt rates would suggest that Fimbulisen has a significantly negative mass balance. The net loss of around 50 km³/a would imply a thinning rate of close to 1 m/a averaged over the ice shelf. While rapid and unsustainable over periods longer than

~100 years, thinning of this order of magnitude has recently been observed in the western Weddell Sea [Shepherd *et al.*, 2003].

[75] If the modeled melt rates are approximately correct, Fimbulisen has a significantly negative net mass balance. Such a situation could not have persisted for more than a few decades, otherwise thinner areas of the ice shelf would already have disappeared. However, an event occurred in 1967 that could possibly have triggered a regime change. Prior to that the thicker central part of the ice shelf, derived from the outflow from Jutulstraumen extended approximately 100 km farther north. This massive ice tongue, named Trolltunga, calved in 1967 as a result of being hit by another massive iceberg that calved from the Amery Ice Shelf a few years earlier [Swithinbank *et al.*, 1977]. Presumably such an event had a profound impact on the local structure of the coastal current and the associated undercurrent. Thus the calving event could conceivably have triggered a regime change within the sub-ice-shelf cavity, with the postcalving undercurrent carrying warm water in as simulated in the model.

[76] Our basal melt rates are based on ocean temperatures at the model domain boundaries that are constant in time, so no account has been taken of the warming trend in the WDW over the two last decades [Smedsrud, 2005]. The maximum core temperature of the WDW within the model domain compares with observed temperatures in the 1980s. The WDW warming since then is likely to further increase basal melting of Fimbulisen.

5. Conclusion

[77] In this study we have analyzed an 11-year simulation from a high-resolution numerical model of the cavity beneath Fimbulisen and the waters to its north. The most significant model result is the simulated southward flow of WDW over a sill at 570 m depth and subsequently beneath Fimbulisen. The presence of warm water in the cavity leads to high levels of basal melting, in excess of 10 m/a in areas close to the grounding line, and an average melting over the central parts of the ice shelf close to 1.9 m/a. The southward inflow of warm water is a compensating flow that balances the northward outflow of fresh, cold water produced by the basal melting.

[78] The model results compare well with observed hydrography and flow. The modeled upper boundary of the WDW on the continental slope, and farther to the north, is found between 400 and 500 m depth. The few observations available for validation indicate that a depth of 500 m is normal, although at other times the WDW can be found as shallow as 370 m, or as deep as 900 m. It is presently not clear from the observations if this reflects a variability in time or space, but is probably a mixture of both. The modeled inflow of WDW below Fimbulisen cannot be validated at present, and yet remains the single most important factor in determining the high melt rates predicted by the model.

[79] What is clear from our analysis of a high-resolution, numerical simulation of the Fimbulisen cavity is that current basal melting of Fimbulisen could be high enough to induce a negative mass balance in the ice shelf and have a major impact on the large-scale oceanography of the Weddell Sea.

The melt rate is controlled primarily by the ease with which WDW accesses the cavity. At present we lack the observations that would tell us for certain if the rate of WDW inflow simulated in the model is realistic. Filling this gap in the observational database must be seen as a high priority, particularly given the recent warming trend of WDW over the last 25 years. If sustained, this trend would lead to even higher basal melting in the future.

[80] **Acknowledgments.** This research was supported by the Norwegian Research Council under contract 143106/432 and by the Bjerknes Centre for Climate Research. This work has received financial support from NASA (grant NAG-5-12419) and the Office of Polar Programs of the U.S. National Science Foundation (grants OPP-9984966 and OPP-0337073). This is publication A 106 of the Bjerknes Centre for Climate Research.

References

- Adcock, S. T., and D. P. Marshall (2000), Interactions between geostrophic eddies and the mean circulation over large-scale bottom topography, *J. Phys. Oceanogr.*, *30*(12), 3223–3238.
- Beckmann, A., and H. Goosse (2003), A parameterization of ice shelf-ocean interaction for climate models, *Ocean Modell.*, *5*, 157–170.
- Bleck, R. (1998), Ocean modelling in isopycnic coordinates, in *Ocean Modelling and Parameterization*, edited by E. Chassignet and J. Verron, pp. 423–448, Kluwer Acad., Norwell, Mass.
- Budd, W. F., and R. Warner (1996), A computer scheme for rapid calculations of balance-flux distributions, *Ann. Glaciol.*, *23*, 21–27.
- Clarke, A. J. (1978), On wind-driven quasi-geostrophic water movements near fast-ice edges, *Deep Sea Res.*, *25*, 41–51.
- Fahrbach, E., R. Peterson, and G. Rohardt (1994), Suppression of bottom water formation in the southeastern Weddell Sea, *Deep Sea Res. Part I*, *41*(2), 389–411.
- Foldvik, A., T. Gammelsrød, and T. Tørresen (1985), Physical oceanography studies in the Weddell Sea during the Norwegian Antarctic Research Expedition 1978/79, *Polar Res.*, *3*, 195–207.
- Gille, S. T. (2002), Warming of the Southern Ocean since the 1950s, *Science*, *295*, 1275–1277.
- Greatbatch, R. J., and G. Q. Li (2000), Alongslope mean flow and an associated upslope bolus flux of tracers in a parameterization of mesoscale turbulence, *Deep Sea Res. Part I*, *47*(4), 709–735.
- Hellmer, H. (2004), Impact of Antarctic ice shelf basal melting on sea ice and deep ocean properties, *Geophys. Res. Lett.*, *31*, L10307, doi:10.1029/2004GL019506.
- Heywood, K., R. A. Locarnini, R. D. Frew, P. F. Dennis, and B. A. King (1998), Transport and water masses of the Antarctic Slope Front System in the eastern Weddell Sea, in *Ocean, Ice, and Atmosphere: Interactions at the Antarctic Continental Margin*, *Antarct. Res. Ser.*, vol. 75, edited by S. S. Jacobs and R. F. Weiss, pp. 203–214, AGU, Washington, D. C.
- Holland, D. M., and A. Jenkins (1999), Modelling thermodynamic ice-ocean interactions at the base of an ice shelf, *J. Phys. Oceanogr.*, *29*(8), 1787–1800.
- Holland, D. M., and A. Jenkins (2001), Adaption of an isopycnic coordinate ocean model for the study of circulation beneath ice shelves, *Mon. Weather Rev.*, *129*(8), 1905–1927.
- Isaksson, E., M. van den Broeke, J. Winther, L. Karlf, J. Pinglot, and N. Gundestrup (1999), Accumulation and proxy-temperature variability in Dronning Maud Land, Antarctica, determined from shallow firn cores, *Ann. Glaciol.*, *29*, 17–22.
- Khazendar, A., and A. Jenkins (2003), A model of marine ice formation within Antarctic ice shelf rifts, *J. Geophys. Res.*, *108*(C7), 3235, doi:10.1029/2002JC001673.
- Klatt, O., E. Fahrbach, M. Hoppema, and G. Rohardt (2005), The transport of the Weddell Gyre across the Prime Meridian, *Deep Sea Res. Part II*, *52*, 513–528.
- Lytche, M. B., and D. G. Vaughan (2001), BEDMAP: A new ice thickness and subglacial topographic model of Antarctica, *J. Geophys. Res.*, *106*(B6), 11,335–11,351.
- Nost, O. A. (2004), Measurements of ice thickness and seabed topography at Fimbul Ice Shelf, Dronning Maud Land, Antarctica, *J. Geophys. Res.*, *109*, C10010, doi:10.1029/2004JC002277.
- O'Dwyer, J. (2002), Report from NARE cruise 2001, *Tech. Rep.*, Norwegian Polar Institute, Tromsø.
- Olbers, D., V. Gouretzki, G. Seiss, and J. Schröter (1992), The hydrographic atlas of the Southern Ocean, Alfred Wegener Inst., Bremerhaven. (Available at <http://www.awi-bremerhaven.de/Atlas/SO>.)
- Orheim, O., J. O. Hagen, S. Østerhus, and A. C. Saetang (1990), Glaciological and oceanographical studies on Fimbulisen during NARE 1989/

- 90, in *Filchner-Ronne Ice Shelf Programme (FRISP), Rep. 4*, edited by H. Oerter, pp. 120–129, Alfred Wegener Inst., Bremerhaven.
- Østerhus, S., and O. Orheim (1992), Studies through Jutulgryta, Fimbulisen, in the 1991/92 season, in *Filchner-Ronne Ice Shelf Programme (FRISP), Rep. 6*, edited by H. Oerter, pp. 103–109, Alfred Wegener Inst., Bremerhaven.
- Rignot, E., and S. Jacobs (2002), Rapid bottom melting widespread near antarctic ice sheet grounding lines, *Science*, 296, 2020–2023.
- Robertson, R., M. Visbeck, A. Gordon, and E. Fahrbach (2002), Long-term temperature trends in the deep waters of the Weddell Sea, *Deep Sea Res. Part II*, 49, 4791–4806.
- Shepherd, A., D. Wingham, A. Payne, and P. Skvarca (2003), Larsen ice shelf has progressively thinned, *Science*, 302(5646), 856–859.
- Smedsrud, L. H. (2005), Warming of the deep water in the Weddell Sea along the Greenwich meridian: 1977–2001, *Deep Sea Res. Part I*, 52(2), 241–258, doi:10.1016/j.dsr.2004.10.004.
- Smedsrud, L. H., A. Jenkins, D. M. Holland, and O. A. Nøst (2005), Ocean processes below Fimbulisen—Modelling results, in *Forum for Research into Ice Shelf Processes (FRISP), Rep. 16*, pp. 43–51, edited by L. Smedsrud, Bjerknes Cent. for Clim. Res., Bergen, Norway.
- Sverdrup, H. U. (1953), The currents off the coast of Queen Maud Land, *Nor. Geogr. Tidsskr.*, 14, 239–249.
- Swithinbank, C., P. McClain, and P. Little (1977), Drift tracks of antarctic icebergs, *Polar Record*, 18(116), 495–501.
- Young, N. W. (1998), Antarctic iceberg drift and ocean currents derived from scatterometer image series, in *ESA-Eumetsat Workshop; Emerging Scatterometer Applications—From Research to Operations, SP-424*, pp. 125–132, ESTEC, Noordwijk, Netherlands.
- Zwally, H. J., J. C. Comiso, C. L. Parkinson, D. J. Cavalieri, and P. Gloersen (2002), Variability of Antarctic sea ice 1979–1998, *J. Geophys. Res.*, 107(C5), 3041, doi:10.1029/2000JC000733.

D. M. Holland, Courant Institute of Mathematical Sciences, New York University, 251 Mercer Street, MC 0711, NY 10012, USA. (holland@cims.nyu.edu)

A. Jenkins, British Antarctic Survey, High Cross, Madingley Road, Cambridge CB3 0ET, UK. (ajen@bas.ac.uk)

O. A. Nøst, Norwegian Polar Institute, Polarmiljøseneteret, N-9296 Tromsø, Norway. (ole.anders.nost@npolar.no)

L. H. Smedsrud, Geophysical Institute, University of Bergen, Allegaten 70, N-5007 Bergen, Norway. (larsh@gfi.uib.no)